SAND2017-9994J

Shock-Ramp Compression of Tin Near the Melt Line

Christopher T. Seagle[1, a)] and Andrew J. Porwitzky[1, b)]

[1]Sandia National Laboratories, Albuquerque, NM 87185, USA

[a)]Corresponding author: ctseagl@sandia.gov
[b)]ajporwi@sandia.gov

Abstract. Tin has been shock compressed to ~69 GPa on the Hugoniot using Sandia's Z Accelerator. A shockless compression wave closely followed the shock wave to ramp compress the shocked tin and probe a high temperature quasi-isentrope near the melt line. A new hybrid backwards integration – Lagrangian analysis routine was applied to the velocity waveforms to obtain the Lagrangian sound velocity of the tin as a function of particle velocity. Surprisingly, an elastic wave was observed on initial compression from the shock state. The presence of the elastic wave indicates tin possess a small but finite strength at this shock pressure, strongly indicating a (mostly) solid state. High fidelity shock Hugoniot measurements on tin sound velocities in this stress range may be required to refine the shock melting stress for pure tin.

INTRODUCTION

Tin (Sn) is a metallic element which has attracted significant attention from the scientific community in regards to its high-pressure behavior, particularly under dynamic loading. A wealth of Hugoniot, shockless compression, and "off-principal" dynamic compression data exist and have been utilized to build multi-phase equation of state models. Existing data and theoretical calculations on the melting of tin on the shock adiabat show wide discrepancy of the melting pressure range on the Hugoniot. Several studies examining the bulk and longitudinal sound speed on the Hugoniot have suggested incipient to complete melting occurs from ~40 – 70 GPa [1], and ~60 – 90 GPa [2]. A similar disagreement is observed in theoretical and modeling research; ranges from ~35 – 55 GPa [3] and ~50 – 65 GPa [4] are reported.

The response of liquid tin to shockless compression is required to build accurate multi-phase equation of state models and helps to define the melt line at high pressures. For several years, Sandia has worked on measuring the response of liquid metals to shockless compression by utilizing shock-ramp techniques [5, 6] on the Z Accelerator [7]. In these experiments, a sample is shock melted and then shocklessly compressed from the Hugoniot state. For application to tin, the initial shock stress of the experiment is particularly challenging to design given the literature discrepancy on the pressure of completion of shock melting on the Hugoniot. A previous study on shock-ramp compression of tin utilized an initial shock of ~65 GPa and the analysis techniques available at that time required an assumed form for the equation of state [6], preventing observation of any elastic response. An additional experiment has now been conducted, with a design shock stress of ~70 GPa. Further improvements of the shock-ramp analysis technique relax the assumption of an assumed form of the equation of state and allow direct measurement of the sound velocity. These advances have allowed examination of the state of the shocked material based on whether elastic behavior, and hence strength, is exhibited on shockless loading from the Hugoniot state. Intentionally sub-solidus shock-ramp experiments on Z have shown that many materials exhibit elastic wave velocities, followed by yielding and plastic flow, from an initial state on the Hugoniot [5]. This is consistent with the shocked material supporting a shear stress at the Hugoniot state.

EXPERIMENT

A shock-ramp experiment was conducted on Sandia's Z Accelerator facility. The hardware consisted of copper stripline panels with a flight gap of 0.25 mm. Tin samples (ρ_0 = 7.29 g/cm^3) of order ~1 mm thickness and lateral dimensions of 7.3 x 8.0 mm were installed on the flight gap shelf, resting above the diamond turned floor of the flyer plate. The samples were backed by lithium fluoride (LiF) windows that were spot coated with 2500 Å aluminum, which was used as a reflector for the VISAR diagnostic [8]. A "double-ramp" pulse shape was designed and generated by the machine. The double-ramp pulse shape is intended to accelerate the panel floors (the flyer) shocklessly to a quasi-ballistic velocity of 3.0 km/s at which point the flyer impacts the tin samples. A "hold" in the current pulse results in a quasi-steady shock imparted to the tin samples. Shortly after impact, the current pulse continues to rise imparting a shockless compression wave into the panels which transfers through the backward moving shock in the flyer and into the samples. The hold duration is designed such that the ramp compression wave closely follows the shock wave in the samples, but does not catch up to the shock within the samples. The measured velocity profiles consist of a shock jump, resulting from the impact, followed by shockless acceleration of the sample-window interface. A cartoon of the experimental hardware configuration and the measured true velocities from one of the sample pairs in shown in Figure 1. The apparent velocities have been corrected for the LiF index to true velocities using a non-linear LiF index model for 532 nm [9].

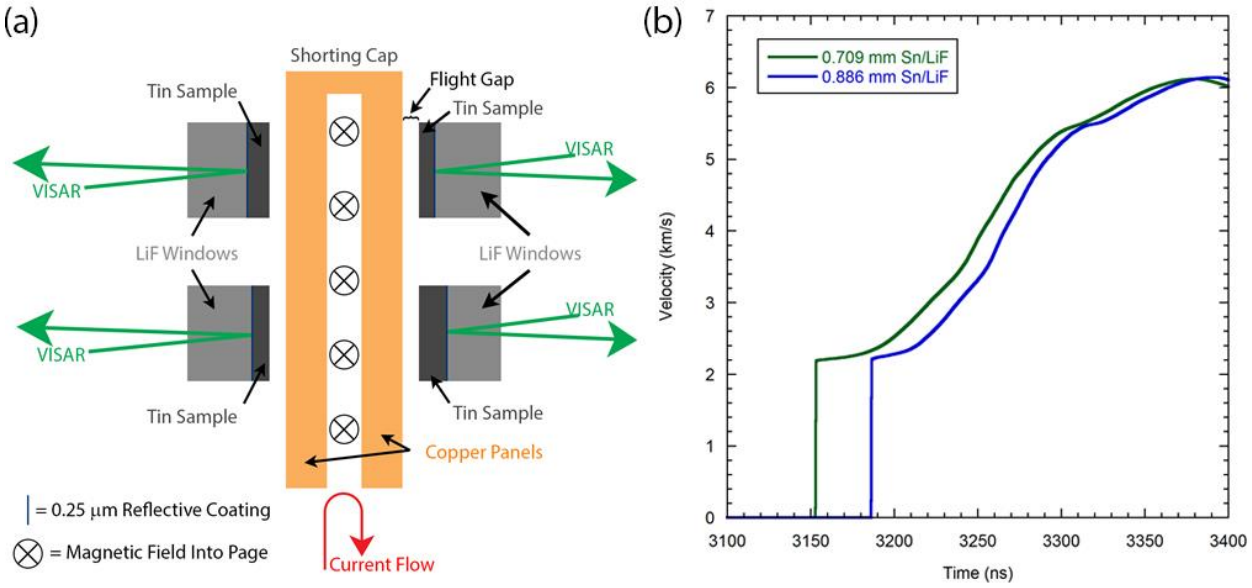

FIGURE 1. a) Cartoon of stripline shock-ramp hardware for the tin experiment. b) Measured true velocities of the tin-LiF interface for one of the sample pairs.

ANALYSIS

The analysis of velocimetry data from shockless compression experiments typically rely on either a characteristics approach [10] or a backward integration approach [11]. In both cases, the technique is necessary to correct measured velocities for free-surface or window-interface wave reflections. In other words, measured velocities almost always differ from the in-situ material velocity due to mechanical wave reflections at the sample boundary. In-situ particle velocities are required for a stress-density analysis of the wave profiles; the technique of iterative Lagrangian analysis (ILA) is typically employed for the analysis of shockless compression experiments. ILA involves propagating the observed wave profiles backwards in space utilizing either the method of characteristics or backwards integration of the hydrodynamic equations. Analysis of shock-ramp wave profiles requires a modified ILA technique which explicitly treats the shock wave characteristic as a boundary condition on the hydrodynamic equations [6]. The following discussion focuses on the backward integration technique as applied

to shock-ramp experiments to obtain in-situ particle velocities from measured sample-window or sample free surface velocity histories.

The Lagrangian form of the hydrodynamic equations are reproduced below as equations (1) and (2).

$$\frac{\partial[P(\rho)]}{\partial x} = -\rho_0 \frac{\partial u}{\partial t} \tag{1}$$

$$\frac{1}{\rho_0}\frac{\partial u}{\partial x} = \frac{\partial[1/\rho]}{\partial t} \tag{2}$$

A direct integration of these equations backward in space as applied to the shock-ramp problem will result in an unphysical solution as the shock at the window boundary disperses into a ramp in the bulk of the sample. To overcome this difficulty, the Hugoniot state, which is assumed known or measured independently in an experiment, must be mathematically forced along the leading shock wave characteristic. This is accomplished by applying a Hugoniot state boundary condition on the shock wave characteristic. The shock characteristic is sloped in (x,t) space, therefore the Lagrangian position of this boundary condition depends on time. By applying a change of variables to the hydrodynamic equations the solution space of interest becomes rectilinear. The change of variables approach is robust and in principal can correctly handle more complex loading paths such as a growing shock followed by a ramp; for example the shock wave characteristic need not be a straight line in (x,t) space. If the shock growth in an experiment is known or measured, a curved shock characteristic with stress and density growing along with the wave in space may be directly applied as a boundary condition with the change of variables approach.

Taking a spatial coordinate $q = q(x)$ and a time coordinate $\tau = \tau(x, t)$, the general form of the Lagrangian hydrodynamic equations becomes:

$$\frac{\partial[P(\rho)]}{\partial q}\left[\frac{dq}{dx} + \frac{\partial \rho}{\partial \tau}\left(\frac{\partial \rho}{\partial q}\right)^{-1}\frac{\partial \tau}{\partial x}\right] = -\rho_0 \frac{\partial u}{\partial \tau}\frac{\partial \tau}{\partial t} \tag{3}$$

$$\frac{1}{\rho_0}\left[\frac{\partial u}{\partial q}\frac{dq}{dx} + \frac{\partial u}{\partial \tau}\frac{\partial \tau}{\partial x}\right] = \frac{\partial[1/\rho]}{\partial \tau}\frac{\partial \tau}{\partial t} \tag{4}$$

In the special case of a steady shock, which launches into a sample of thickness x_T, at time t_0, and propagates at shock velocity U_s, one can define $q = x/x_T$ and $\tau = [x+U_s(t_0\text{-}t)]/[x+U_s(t_0\text{-}t_f)]$, where t_f is the final time of interest chosen well after peak stress/velocity at the free surface or sample-window interface. Equations (3) and (4) then become:

$$\frac{\partial[P(\rho)]}{\partial q}\left[\frac{1}{x_T} + \frac{\partial \rho}{\partial \tau}\left(\frac{\partial \rho}{\partial q}\right)^{-1}\frac{\tau - 1}{U_s(t_f - t_0) - qx_T}\right] = \rho_0 \frac{\partial u}{\partial \tau}\frac{U_s}{U_s(t_0 - t_f) + qx_T} \tag{5}$$

$$\frac{1}{\rho_0}\left[\frac{1}{x_T}\frac{\partial u}{\partial q} + \frac{\partial u}{\partial \tau}\frac{\tau - 1}{U_s(t_f - t_0) - qx_T}\right] = -\frac{\partial[1/\rho]}{\partial \tau}\frac{U_s}{U_s(t_0 - t_f) + qx_T} \tag{6}$$

In the Hugoniot state, the particle velocity is u_p^H and the density is ρ^H. With these definitions and a measured free surface velocity, $u_b(t) \leftrightarrow u_b(\tau)$, the boundary conditions applied to equations (5) and (6) are:

$$
\begin{aligned}
u(1,\tau) &= u_b(\tau) \\
u(q,0) &= \begin{cases} u_p^H \text{ if } q<1 \\ u_b(0) \text{if } q=1 \end{cases} \\
\rho(1,\tau) &= \begin{cases} \rho_0^R \text{ if free surface} \\ \rho_b(\tau) \text{if windowed} \end{cases} \\
\rho(q,0) &= \begin{cases} \rho^H \text{ if } q<1 \\ \rho_0^R \text{ if } q=1 \,\&\, \text{free surface} \\ \rho_b(0) \text{if } q=1 \,\&\, \text{windowed} \end{cases}
\end{aligned}
\tag{7}
$$

For a windowed experiment, the former two boundary conditions on density can be found by impedance matching with the known window equation of state. Note that ρ_0^R is not the Standard Temperature Pressure (STP) density, but rather the release density at zero pressure from the Hugoniot state. This release density falls on the same isentrope as the shock-ramped material. Equations (5), (6), and (7) may be used with a guess of the equation of state of the sample to derive an in-situ velocity history by integrating to position q=0 and utilizing the density/velocity history at this position to propagate the waves forward in space using characteristics [10] up to the thickness of the samples as if no window were present. With these in-situ velocities, a Lagrangian sound speed analysis may be used to define a new equation of state and the whole procedure repeated until convergence. Note that one must reverse the change of variables back to standard Lagrangian coordinates before propagating the waves forward and performing a Lagrangian sound speed analysis.

This procedure was applied to the tin velocities measured on the Z experiment, the LiF equation of state used was 7271v3 [5, 12]. The converged Lagrangian sound velocity as a function of particle velocity is displayed in Figure 2. Immediately clear is the elastic wave velocity on initial compression from the Hugoniot state, subsequently yielding, and an increase in the bulk wave velocity follow. Tin apparently exhibits strength at this shock stress (69.2 ± 0.3 GPa), where several studies suggest it should be fully melted. Presumably, for a partially molten material to exhibit strength, the melt fraction must be less than some critical value which results in the solid component remaining connected through the thickness of the sample. Although it is not possible to directly extract a strength measurement from the measured sound velocities, the change in shear stress using equation (9b) of Huang and Asay, 2005 [13] is 0.45 ± 0.20 GPa, indicating a small but finite support for shear stress.

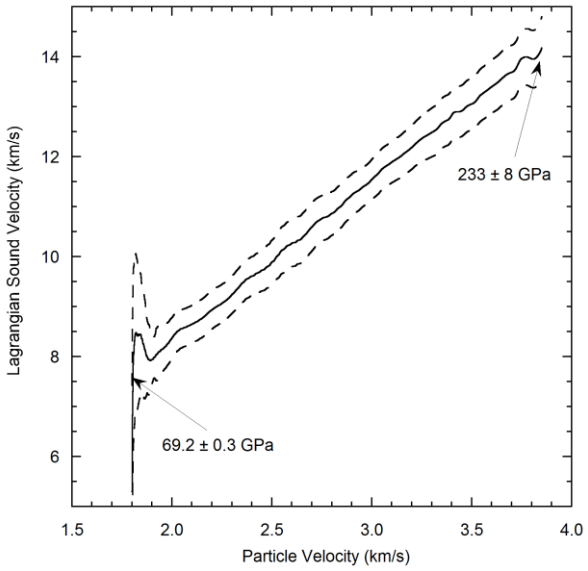

FIGURE 2. Lagrangian sound velocity of tin as a function of particle velocity on shockless compression from an initial shock state of 69.2 ± 0.3 GPa. The elastic behavior between a particle velocity of ~1.8 – 1.9 km/s indicates the tin exhibits strength at this shock stress and is therefore at least partially solid.

DISCUSSION

There is a large discrepancy on the stress range over which tin melts on the Hugoniot. Improvements in the analysis techniques of shock-ramp velocimetry data have allowed relaxation of previous assumptions regarding the form of the equation of state. Sample response can be determined directly using a hybrid "backward integration-characteristic-Lagrangian analysis". This technique, as applied to the tin shock-ramp data presented, has demonstrated nearly linear response in the sound velocity – particle velocity plane and that tin is at least partially solid at ~69 GPa, evidenced by the support of shear stress. Several studies predict complete melting should have occurred at this Hugoniot stress. Additional sound speed data on the Hugoniot in the ~40 – 100 GPa stress range would be helpful in further addressing the shock melting of this metal. Future Z shock-ramp experiments are planned utilizing higher initial shock stresses to search for signs of loss of strength on the Hugoniot and possibly strength on unloading due to re-solidification during shockless compression from an initially completely molten state.

ACKNOWLEDGMENTS

The authors thank the large team at Sandia required to design, fabricate, and field experiments on the Z Accelerator. Sandia National Laboratories is a multi-mission laboratory managed and operated by National Technology and Engineering Solutions of Sandia LLC, a wholly owned subsidiary of Honeywell International Inc. for the U.S. Department of Energy's National Nuclear Security Administration under contract DE-NA0003525.

REFERENCES

1. Hu, J., et al., *Successive phase transitions of tin under shock compression.* Appl. Phys. Lett., 2008. **92**: p. 111905.
2. Zhernokletov, M.V., et al., *Measurement of the sound velocities behind the shock wave front in tin.* Combustion, Explosion, and Shock Waves, 2012. **48**: p. 112-118.
3. Cox, G.A., *A multi-phase equation of state and strength model for tin.* AIP Conf. Proc. , 2006. **845**: p. 208.
4. Khishchenko, K.V., *Equation of state and phase diagram of tin at high pressures.* J. Physics: Conf. Series, 2008. **121**: p. 022025.
5. Seagle, C.T., J.-P. Davis, and M.D. Knudson, *Mechanical response of lithium fluoride under off-principal dynamic shock-ramp loading.* J. Appl. Phys., 2016. **120**: p. 165902.
6. Seagle, C.T., et al., *Shock-ramp compression: Ramp compression of shock-melted tin.* Appl. Phys. Lett., 2013. **102**: p. 244104.
7. Reisman, D.B., et al., *Magnetically driven isentropic compression experiments on the Z accelerator.* J. Appl. Phys., 2001. **89**: p. 1625-1633.
8. Barker, L.M. and R.E. Hollenbach, *Laser interferometer for measureing high velocities of any reflecting surface.* J. Appl. Phys., 1972. **43**: p. 11.
9. Rigg, P.A., et al., *Determining the refractive index of shocked [100] lithium fluoride to the limit of transmissibility.* J. Appl. Phys., 2014. **116**: p. 033515.
10. Rothman, S.D. and J. Maw, *Characteristics analysis of isentropic compression experiments.* J. Phys. IV France, 2006. **134**: p. 745.
11. Hayes, D., *Backward integration of the equations of motion to correct for free surface perturbations.* Sandia Report, 2001. **SAND2001-1440**.
12. Davis, J.-P., et al., *Mechanical and optical response of [100] lithium fluoride to multi-megabar dynamic pressures.* J. Appl. Phys., 2016. **120**: p. 165901.
13. Huang, H. and J.R. Asay, *Compressive strength measurements in aluminum for shock compression over the stress range of 4 - 22 GPa.* J. Appl. Phys., 2005. **98**: p. 033524.